Effect of dispersive conductivity and permittivity in volume conductor models of deep brain stimulation

Peadar F. Grant, *Student Member, IEEE*, and Madeleine M. Lowery, *Member, IEEE*

***Abstract*—The aim of this study was to examine the effect of dispersive tissue properties on the volume conducted voltage waveforms and volume of tissue activated during deep brain stimulation. Inhomogeneous finite-element models were developed, incorporating a distributed dispersive electrode-tissue interface and encapsulation tissue of high and low conductivity, under both current-controlled and voltage-controlled stimulation. The models were used to assess the accuracy of capacitive models, where material properties were estimated at a single frequency, with respect to the full dispersive models. The effect of incorporating dispersion in the electrical conductivity and relative permittivity was found to depend on both the applied stimulus and the encapsulation tissue surrounding the electrode. Under current-controlled stimulation, and during voltage-controlled stimulation when the electrode was surrounded by high resistivity encapsulation tissue, the dispersive material properties of the tissue were found to influence the voltage waveform in the tissue, indicated by RMS errors between the capacitive and dispersive models of 20% to 38% at short pulse durations. When the dispersive model was approximated by a capacitive model, the accuracy of estimates of the volume of tissue activated was very sensitive to the frequency at which material properties were estimated. When material properties at 1 kHz were used, the error in the volume of tissue activated by capacitive approximations was reduced to -4.33% and 11.10% respectively for current-controlled and voltage-controlled stimulation, with higher errors observed when higher or lower frequencies were used.**

***Index Terms*—Deep brain stimulation, computational model, dispersion, capacitance**

I. Introduction

DEEP brain stimulation (DBS) is a highly effective therapy for treating the symptoms of many neurological conditions, including Parkinson's disease, essential tremor and dystonia [1]. Despite its success, the mechanisms of action of DBS remain poorly understood [2]. Stimulus parameter selection for each subject is, therefore, a time-consuming process, currently performed by trial-and-error [3]. Computational models have been found to be an effective way to investigate the mechanisms of action of DBS. Additionally, the use of such models to aid parameter selection can improve the efficacy of the stimulus and reduces the time taken for stimulus programming whilst minimising side effects [4].

Analytical and numerical volume conduction models of deep brain stimulation allow the electric potential in the surrounding neural tissue to be estimated. Such models have been applied to predict the shape and extent of neural activation [5], and to evaluate the performance of different electrodes and stimulation waveforms [6]. Modelling advances have allowed various volume conduction effects to be quantified, such as encapsulation tissue electrical properties [7], tissue anisotropy [8], localised tissue inhomogeneities and anisotropies [9] and electrical grounding [10], [11].

It is well established that the electrical conductivity and relative permittivity of many biological tissues, including grey matter and white matter are dispersive, that is they vary as a function of frequency [12]. Historically, most bioelectric volume conductor models have applied the quasi-static approximation, which assumes that capacitive, inductive and propagation effects may be ignored [13]. A limited number of DBS models have incorporated displacement currents within the tissues surrounding the electrode [6], [14], concluding that capacitive effects may be clinically significant under current-controlled stimulation. However, these models have not considered the frequency-dependent nature of the electrical properties of biological tissues. Dispersive electrical conductivity and relative permittivity have been incorporated in a homogeneous analytical model, considering a point current stimulus in infinite space [15]. Although parametric models for the frequency-dependent material properties of many biological tissues are available [12], the influence of dispersion in inhomogeneous models of deep brain stimulation has not yet been examined for both current and voltage-controlled stimulation nor for electrode encapsulation tissue of varying properties.

Recent advances in implantable stimulation technology now allow current-controlled stimulation to be applied in human subjects, in addition to voltage-controlled stimulation which is clinically used at present [16]. With a small number of exceptions, [6], [15], the majority of volume conductor DBS models to date focused on voltage-controlled stimulation. Modelling studies suggest that a re-examination of frequency-dependent volume conduction effects may be necessary in the context of current-controlled stimulation, under which capacitive effects, generally assumed to be negligible, may be clinically significant [6], [17].

The aim of this study was to quantify dispersive tissue effects in an inhomogeneous model of DBS, and to investigate whether a resistive or capacitive model with fixed material properties could provide a good approximation to the full dispersive model when estimating voltage waveforms and resulting volumes of activation. To address this question, a frequency domain model incorporating dispersion in an

This work was funded by Science Foundation Ireland under research grant number 05/RF/ENM047.

***Corresponding author information:** Peadar Grant UCD School of Electrical, Electronic and Mechanical Engineering Belfield, Dublin 4, Ireland.* E-mail: peadargrant@me.com

inhomogeneous volume conductor was developed. The model presented considers an idealised whole-head geometry, a three-dimensional stimulation electrode, the electrical double-layer at the electrode-tissue interface, variations in the electrode encapsulation tissue and dispersive tissue properties for both current-controlled and voltage-controlled stimuli. The volume of tissue activated was estimated using an embedded axon cable model [5], and compared among current and voltage-controlled stimulation with highly resistive and conductive encapsulation regions.

II. Methods

An idealised ellipsoidal geometry was used to represent the intracranial conducting volume of an adult human head [10]. This geometry allowed the effects electrical grounding associated with DBS to be incorporated into the model whilst retaining a reduced computational complexity relative to subject-specific geometries [9], [11]. Similar idealized geometries have been commonly employed in other fields, notably electroencephalography [18]. The semi-axes of the intracranial conducting volume were 70 mm, 82.5 mm and 65 mm in the medial-lateral, anterior-posterior and superior-inferior directions respectively. The brain tissue was encased within the skull which consisted of a 4.5 mm thick layer of cortical bone. This was covered by the scalp, composed of a layer of 5.5 mm thick non-infiltrated fat tissue. The cerebrospinal fluid was represented by a uniform 1.78 mm thick layer enclosed by the skull.

A Medtronic 3387 electrode [19], radius 0.635 mm and contact height 1.5 mm, was simulated to lie within in the model, as described in [10]. An encapsulation layer 0.2 mm thick was included to allow resulting material property changes resulting from the formation of collagen, fibroblasts and giant cells, as well as highly conductive fluid present during the acute post-operative phase to be incorporated [7], [14]. The boundary at which the spinal cord enters the skull was designated as the electrical reference surface or ground.

A. Material properties

Tissue properties for brain tissue, skull bone and scalp were assigned based on values reported by Gabriel *et al* [12]. The brain region was assumed to consist of homogeneous isotropic grey matter. The conductivity of cerebrospinal fluid was taken to be $1.6\,\mathrm{S\,m^{-1}}$ [20], and its relative permittivity to be 200 [21]. Material properties were spatially invariant within each region.

The encapsulation layer surrounding the electrode was modelled under three different conditions: with material properties equal to grey matter, with conductivity higher than grey matter to simulate conditions where the electrode has been implanted for some time and with conductivity lower than grey matter to simulate conditions where the electrode has been recently implanted [7], [14]. In the high conductivity case, the encapsulation region consisted of purely conductive cerebrospinal fluid [14]. In the high resistivity case the encapsulation region consisted of purely resistive tissue of conductivity $0.0125\,\mathrm{S\,m^{-1}}$.

B. Governing equations

The system was governed by the time-harmonic formulation of the Laplace equation, where ϕ is the electric potential, considered for three mathematical representations of the volume conductor: resistive, capacitive and dispersive.

In the resistive case only conduction currents were considered:

$$-\nabla\cdot\sigma(\omega_c)\nabla\phi = 0 \tag{1}$$

where σ denotes the electrical conductivity, estimated at the constant angular frequency ω_c. The capacitive case considered also the displacement currents:

$$-\nabla\cdot[\sigma(\omega_c)+j\omega\epsilon_0\epsilon_r(\omega_c)]\nabla\phi = 0 \tag{2}$$

where σ denotes the electrical conductivity and ϵ_r the relative permittivity, which were both estimated at the angular frequency ω_c. In this study, the electrical conductivity and the relative permittivity for the resistive and capacitive models were evaluated at 1000 Hz, approximately the median frequency of a typical DBS waveform. It was assumed that inductive and propagation effects were negligible for the combination of the wavelengths of the stimulus waveform and the dimensions of the volume conductor. When estimating volume of activation, the material properties were estimated at additional fixed frequencies of 100 Hz and 10 000 Hz.

To fully incorporate dielectric dispersion, at each component frequency the constants defining the electrical conductivity and relative permittivity were replaced by their Cole-Cole dispersion functions as described by Gabriel *et al.* [12]. The response of the system to each component was therefore estimated using the corresponding value of the electrical conductivity and relative permittivity at that frequency, ω.

$$-\nabla\cdot[\sigma(\omega)+j\omega\epsilon_0\epsilon_r(\omega)]\nabla\phi = 0 \tag{3}$$

To separate the effects of dispersion in the conductivity and relative permittivity, the electrical conductivity and relative permittivity were alternately allowed to vary with frequency whilst the other parameter was fixed at its value at 1000 Hz.

$$-\nabla\cdot[\sigma(\omega)+j\omega\epsilon_0\epsilon_r(\omega_c)]\nabla\phi = 0 \tag{4}$$

$$-\nabla\cdot[\sigma(\omega_c)+j\omega\epsilon_0\epsilon_r(\omega)]\nabla\phi = 0 \tag{5}$$

C. Excitations and boundary conditions

In the models using current controlled stimulation, the normal component of the uniform current density crossing the surface of the electrode contact was set to $1\,\mathrm{A\,m^{-2}}$. In the models of voltage controlled stimulation, the electric potential on the boundary surface of the electrode contact was set to 1 V. The reference surface was fixed at zero volts. The normal component of the current density was zero on all exterior boundaries, and was conserved across interior boundaries, satisfying:

$$\hat{\sigma_1}E_{1n} = \hat{\sigma_2}E_{2n} \tag{6}$$

where $\hat{\sigma_1}$ and $\hat{\sigma_2}$ are the complex conductivities, incorporating electrical conductivity and relative permittivity of the regions 1 and 2, and E_{1n} and E_{2n} are the normal components of the electric field in regions 1 and 2.

D. Electrode-tissue interface

The electrical double-layer was implemented using the thin-layer approximation formulation described in [22]. The double-layer equivalent impedance Z_{PE} represents the parallel combination of the pseudo-capacitive constant phase angle element Z_{CPA}, Eq. 7, and the over-potential-independent form of the charge-transfer resistance R_{CT}, Eq. 8 [23].

$$Z_{CPA} = K(j\omega)^{-\beta} \quad (7)$$

$$R_{CT} = \frac{RT}{nFI_O} \quad (8)$$

The double-layer was assumed to be 1 nm thick, where K and β denote physical constants, R the universal gas constant, F Faraday's constant, T temperature, n number of electrons per molecule, and I_O exchange current. Parameter values used were as described by Cantrell *et al.* [22], which were obtained from experimental studies on platinum electrodes [23]. The parallel combination of Z_{CPA} and R_{CT} yielded impedances of 746 Ω, 91 Ω and 11 Ω at 100 Hz, 1000 Hz and 10 000 Hz respectively.

In the voltage controlled stimulus models, the electrical double-layer was implemented using the thin-layer distributed impedance formulation of the thin-layer approximation, where Y_l represents the specific admittance of the double-layer, V_S represents the stimulus voltage, V_T represents the voltage at the tissue and Y_l is the specific admittance of the double-layer. The material properties were spatially invariant within the thin layer.

$$-n \cdot J = (V_S - V_T)Y_l \quad (9)$$

The equivalent capacitances of the double-layer was 2.2 µF, 1.8 µF and 1.4 µF at 100 Hz, 1000 Hz and 10 000 Hz respectively, which lies within the range of electrode capacitance values in previous studies [24], [25]. In the current controlled stimulus models, the electrical double-layer was approximated by a lumped equivalent electrical circuit. It was confirmed that the double-layer had negligible effect under current controlled conditions and it was not included in subsequent models of current controlled stimulation.

The effect of the double layer on the waveform was compared to that observed when the interface was replaced by lumped electrode capacitances of 1.65 µF, 3.3 µF and 6.6 µF as used in previous models [24].

E. Simulation details

The whole head geometry was discretised using the Delaunay free-meshing algorithm into approximately 350,000 tetrahedral elements. Interior and exterior boundary surfaces were meshed using triangles, prior to generation of the tetrahedral element mesh. Linear Lagrange shape functions were extended on to each tetrahedral element to approximate the electric potential, which is the dependent variable. These allowed the solution to predict linear spatial variation of the electric potential within each element [26]. COMSOL Multiphysics 3.5a (COMSOL AB, Stockholm) was used to solve the model at 2000 component frequencies, providing the model transfer function, which estimates the output spectrum at a point 1 mm from the electrode, within the region of the target neurons [20]. Mesh convergence was checked by ensuring that the solution differed by less than 1% when the number of elements was doubled.

The DBS waveform was synthesised in the time domain from 2000 harmonics of the fundamental stimulation frequency using the trigonometric Fourier expansion. The stimulus parameters used monophasic pulses with a stimulation frequency of 130 Hz and a duration of 60 µs, typical of that used clinically [3], except where otherwise stated. The inverse Fourier transform of the product of the stimulus spectrum and the transfer function of the volume conductor was calculated to yield the voltage waveform in the tissue 1 mm from the electrode surface.

F. Estimation the volume of tissue activated

The effect of the simulated waveforms on neural activation was examined using the embedded axon cable model described by McIntyre *et al.* [27], assuming that activation occurs along the axon [28]. Each axon had 21 nodes of Ranvier, and included the paranodal and internodal segments as well as the myelin sheath, as detailed in [27], and lay parallel to the medial-lateral axis. The axons were simulated in the NEURON 7.0 simulation environment, using axon diameter 5.7 µm [29].

Estimation of the volume of tissue activated was performed using 4131 axons arranged in a 51 × 81 grid, with 0.1 mm spacing along the anterior-posterior and superior-inferior axis. The stimulus voltage or current required to elicit action potential propagation in an axon 1.5 mm from the encapsulation region in the fully dispersive tissue model was established. This stimulus was subsequently applied to calculate the closed contour inside which the stimulus will cause activation of an axon perpendicular to the electrode, in a manner similar to previous studies [6]. The contour was then rotated about the central axis of the electrode to calculate the volume of tissue activated. The volumes of tissue activated as predicted by the resistive and capacitive models were then compared to that predicted by the dispersive model for current-controlled and voltage-controlled stimulation, with conductive and highly-resistive encapsulation tissue.

III. Results

The voltage waveform in the tissue following incorporation of the dispersive double layer was compared to that estimated using lumped capacitive approximations, as presented in Fig. 1. The RMS errors of the voltage waveforms estimated using lumped electrode capacitance values of 1.65 µF, 3.3 µF with respect to that estimated when distributed double-layer was incorporated are presented in Table I for the various encapsulation tissue conditions, and were less than 8% in all cases.

The effect of dispersion in the electrical conductivity and relative permittivity of brain tissue under voltage-controlled stimulation was then examined under three separate conditions, as presented in Fig. 2. When the encapsulation tissue was replaced with grey matter, the waveforms were almost

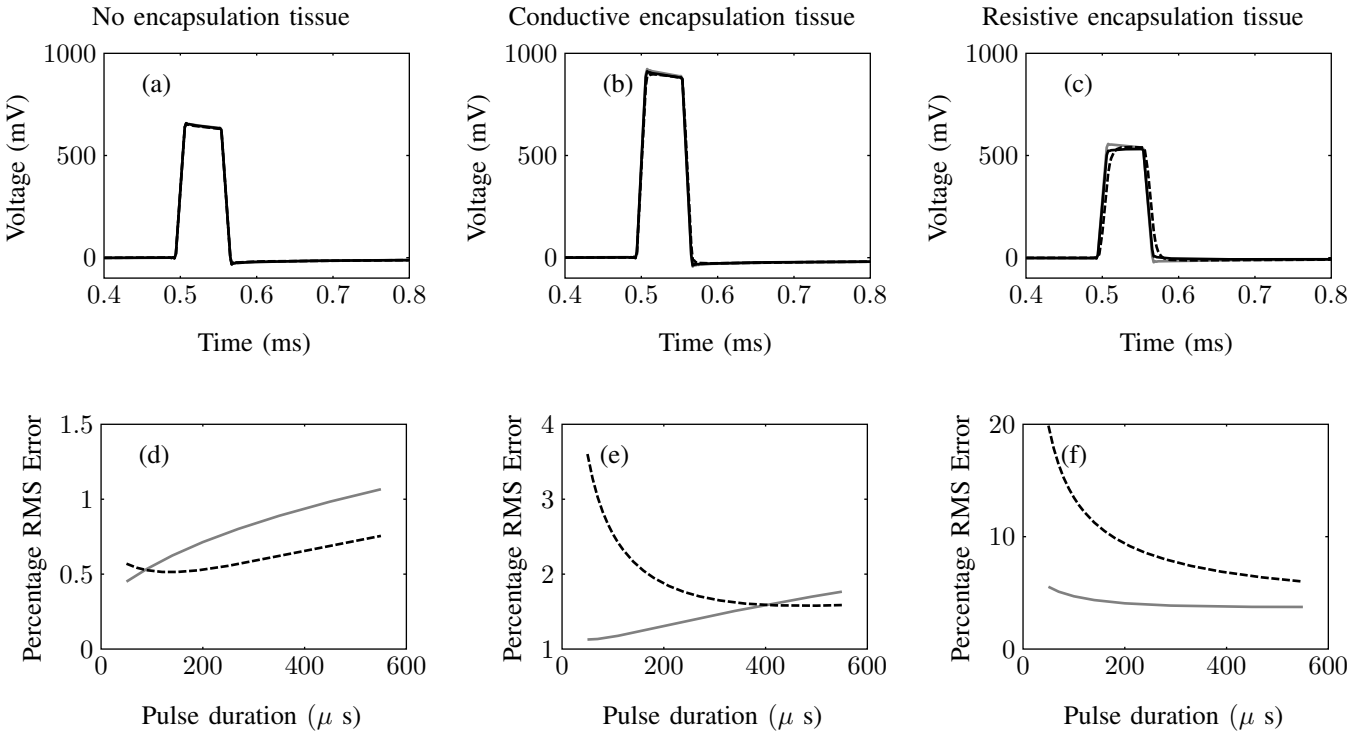

Fig. 2. Simulated voltage waveforms (a, b, c) under voltage controlled stimulation 1 mm from the stimulating electrode contact for resistive (grey line), capacitive (dashed line) and dispersive (solid line) brain tissue properties with (a) encapsulation region filled with grey matter, (b) encapsulation region of higher conductivity than grey matter and (c) encapsulation region of lower conductivity than grey matter. Corresponding percentage root mean square error of resistive and capacitive brain tissue properties at 1 kHz with respect to fully dispersive brain tissue properties (d, e, f) over pulse durations ranging from 50 µs to 550 µs.

TABLE I
RMS ERRORS OF VOLTAGE WAVEFORM IN THE TISSUE ESTIMATED WHEN THE ELECTRODE-TISSUE INTERFACE WAS APPROXIMATED USING LUMPED CAPACITANCES TO THAT ESTIMATED WHEN THE DISTRIBUTED DOUBLE LAYER WAS INCORPORATED.

Encapsulation region	Lumped electrode capacitance		
	1.65 µF	3.30 µF	6.60 µF
Grey matter	4.86%	4.32%	4.87%
Conductive	7.70%	5.54%	5.95%
Resistive	4.13%	3.76%	4.24%

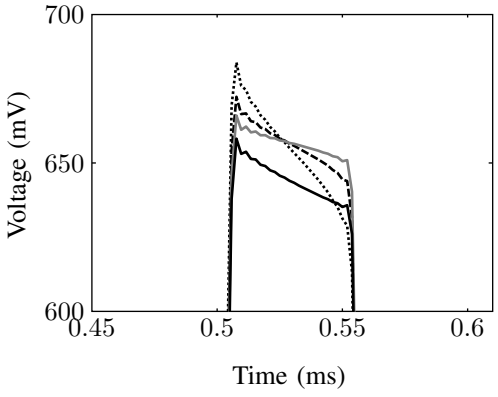

Fig. 1. Comparison of voltage waveform in the tissue resulting from lumped electrode capacitances of 1.65 µF (dotted line), 3.3 µF (dashed line), 6.6 µF (grey line) and distributed double layer (solid line).

identical, Fig. 2(a). Across a range of pulse durations, the root mean squared (RMS) errors of the resistive and capacitive waveforms with respect to the dispersive waveform were less than 1%, Fig. 2(d). When the electrode encapsulation region was filled with cerebrospinal fluid, to approximate the condition post-implantation, the waveforms remained qualitatively similar, Fig. 2(b). In this case, the RMS error of the capacitive waveform, where the electrical conductivity and relative permittivity were estimated at 1 kHz, with respect to the dispersive waveform was higher than that of the resistive waveform, Fig. 2(e). When the electrode was surrounded by resistive encapsulation tissue, the shape of the waveforms varied depending whether the tissue was modelled as resistive, capacitive or dispersive, Fig. 2(c), and RMS errors of up to 20% were observed for short pulse durations, Fig. 2(f).

The simulated voltage waveforms in the whole head geometry predicted by the resistive, capacitive and dispersive models under current-controlled stimulation are presented in Fig. 3(a). RMS errors of up to 38% were observed in the waveforms estimated by the 1 kHz capacitive model with respect to the fully dispersive model at short pulse durations, Fig 3(b). The effect of including dispersive material properties, and the RMS errors which resulted from the use of resistive or capacitive material properties remained unchanged when the encapsulation region was replaced with either conductive cerebrospinal fluid or resistive tissue. The characteristic shapes of the resistive, capacitive and dispersive waveforms, remained constant as the encapsulation tissue properties were varied.

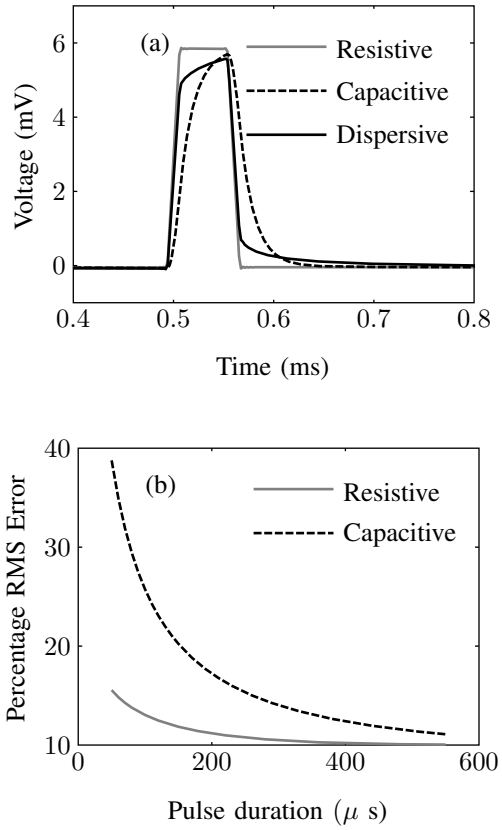

Fig. 3. Simulated voltage waveforms (a) under current controlled stimulation 1 mm from the stimulating electrode contact for resistive, capacitive and dispersive brain tissue properties with encapsulation region filled with grey matter. Corresponding percentage root mean square error (b) of resistive and capacitive brain tissue properties with respect to fully dispersive brain tissue properties as pulse duration was varied.

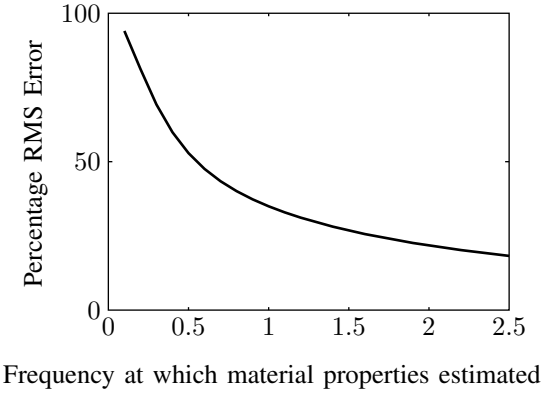

Fig. 4. Percentage root mean square error of voltage waveform resulting from capacitive brain tissue with respect to fully dispersive brain tissue over material properties estimated in the range 100 Hz to 2500 Hz.

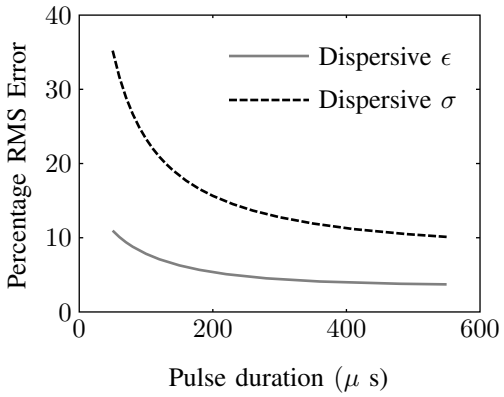

Fig. 5. Percentage root mean square error of voltage waveform resulting from dispersion in electrical conductivity and dispersion in relative permittivity with respect to that resulting from fully dispersive tissue properties as pulse duration was varied.

Neglecting the dispersive material properties by approximating them with a fixed electrical conductivity and relative permittivity value resulted in variations in the characteristic shape of the voltage waveform depending on the frequency value at which the material properties were estimated. As the frequency at which material properties were calculated was increased, the RMS error of the capacitive solution with respect to the dispersive solution decreased, Fig. 4.

The RMS error of the simulated voltage waveforms resulting from dispersion in the electrical conductivity or in the relative permittivity alone with respect to that resulting from the fully dispersive model were up to 35% and 10%, respectively, for pulse durations in the range 50 µs to 550 µs, Fig. 5.

The percentage differences between the volume of tissue activated predicted by the resistive and capacitive models where the material properties were estimated at 1 kHz with respect to the dispersive model are presented in Table II. Use of a purely resistive tissue model under current-controlled stimulation increased the volume of tissue activated by approximately 84.28% compared to a fully dispersive tissue model. When a capacitive model was used, the volume of tissue activated depended on the frequency at which the electrical conductivity and relative permittivity of brain tissue were estimated. Simulations conducted using material properties estimated at 100 Hz, 1000 Hz and 10 000 Hz were found to cause the volume of tissue activated to differ from that predicted using a fully dispersive model by -58.46%, -4.33% and 11.33% respectively under current-controlled stimulation.

The differences in the volume of tissue activated under voltage-controlled stimulation depended on the composition of the encapsulation region as shown in Table II. When the encapsulation region consisted of highly conductive or highly resistive tissue, the volume of tissue activated predicted by the capacitive model with both conductivity and relative permittivity estimated at 1000 Hz was found to be 4.81% less and 12.34% greater, respectively, than that predicted by the fully dispersive model. When the material properties were estimated at 100 Hz and 10 000 Hz in the capacitive model, the volume of tissue activated differed by -99.52% and -4.97% respectively.

IV. Discussion

The purpose of this study was to quantify the effect of frequency dispersion in the electrical properties of brain tissue, under both voltage-controlled and current-controlled stimulation in an inhomogeneous model of DBS. This expanded

TABLE II
PERCENTAGE DIFFERENCES IN THE VOLUME OF TISSUE ACTIVATED IN RESISTIVE AND CAPACITIVE MODELS, COMPARED TO THE FULL DISPERSIVE MODEL. CAPACITIVE AND RESISTIVE TISSUE PROPERTIES WERE CALCULATED AT 1000 Hz.

Applied stimulus	Encapsulation region	Stimulus amplitude	Resistive model	Capacitive model
Current	Grey matter	26.8 A m^{-2}	84.28%	-4.33%
Voltage	Grey matter	0.23 V	0.46%	-2.03%
Voltage	Conductive	0.16 V	11.60%	-5.03%
Voltage	Resistive	0.28 V	21.06%	11.10%

on previous reported results by incorporating the dispersive electrode-tissue interface simultaneously with dispersion in the electrical properties of the brain tissue in a whole-head volume conductor [6], [15]. In previous modeling studies, the dispersive double-layer has been approximated by the insertion of a single lumped electrode capacitance [20], [24]. The equivalent lumped capacitances of the physically-based distributed double layer implemented in this study were found to be within the range of electrode capacitance values reported in previous studies [24], [25]. Additionally, the parameters describing the double-layer yielded impedances within the range of measured experimental values in saline [30]. The double-layer formulation predicted a voltage drop not captured by the lumped capacitive approximations, Fig. 1. In addition, the physically-based double layer allows the physical processes occuring at the electrode interface to be expressed in the model, negating the need to approximate the interface with a single lumped capacitance [22], [23]. If capacitive approximations are substituted for the dispersive double-layer, the results indicate that the RMS error is less than 5.6% when the 3.3 μF capacitance derived for human DBS electrodes is selected, Table I [24].

Under voltage-controlled stimulation, the effect of incorporating frequency dispersion on the waveform and resulting volume of tissue activated depended on the composition of the encapsulation region surrounding the electrode. The results agree with previous studies which examined the effect of incorporating capacitive material properties estimated at a single frequency, for which the high-pass filtering of the electrode-tissue interface dominates over capacitive tissue effects, except when the electrode is surrounded by high-resistivity encapsulation tissue [24], [31]. In the absence of encapsulation tissue, the RMS error of the voltage waveform predicted by the resistive and the non-dispersive capacitive models with respect to the fully dispersive model were less than 1.5% across a range of pulse durations, Fig. 2(d), and the resulting volume of tissue activated differed by less than 2.1% from that estimated using the full dispersive tissue properties, Table II. This suggests that under voltage-controlled stimulation where encapsulation tissue is not present, the quasi-static model with conductivity estimated at 1000 Hz provides a close approximation of the waveforms and volume of tissue activated to that predicted by the full dispersive model. The high-pass filtering effect of the double layer was present in the waveforms predicted by all three tissue models, Fig. 2(a), which is in agreement with previous studies that show that the effect of the electrode interface is dominant over any effect of tissue capacitance under voltage-controlled stimulation in the absence of encapsulation tissue [24].

When the electrode was surrounded by a highly conductive encapsulation region, the RMS error of the voltage waveform predicted by the resistive and the non-dispersive capacitive models, with material properties estimated at 1 kHz, remained below 5% across a range of pulse durations, Fig. 2(e). The volume of tissue activated was 5.03% less when a capacitive model was used compared to when the fully dispersive model was used, but was 11.60% greater when the resistive model was used. This suggests that when the electrode is surrounded by highly conductive fluid, the use of a resistive model may overestimate the volume of tissue activated. This is in agreement with existing literature, which reports a reduction in the maximum radial distance at which action potential propagation will occur when capacitive material properties estimated at a single frequency are introduced [14].

When the encapsulation region was replaced with tissue with a high resistivity to simulate a chronically implanted electrode [14], the RMS errors in the resistive and capacitive waveforms were increased. The high-pass filtering effect of the double-layer was not apparent in the waveforms produced by capacitive or full dispersive models, Table II. The purely resistive tissue model caused the volume of activation to be overestimated by 21.06%, in agreement with previous studies which report a reduction in the volume of tissue activated when capacitive material properties estimated at a single frequency were introduced [14]. The errors in the volume of tissue activated when using the capacitive model where material properties were estimated at 100 Hz, 1000 Hz and 10 000 Hz were found to be -99.52%, 11.10% and -4.97% respectively, suggesting that the magnitude of the error may be reduced by estimating material properties in the range of 1 kHz to 10 kHz.

When current-controlled stimulation was applied, the electrical double-layer had a negligible effect, since the inward current to the volume conductor was explicitly defined and capacitive and dispersive effects dominated the waveform shape, Fig. 3(a). As pulse durations were reduced, the RMS errors between the resistive and capacitive waveforms with respect to the dispersive waveform increased, Fig. 3(b). The dispersive waveforms which resulted were of similar shapes to those reported for homogeneous analytical models that delivered current-controlled stimuli from a single point source in a conducting volume of infinite extent [15], while the tissue waveforms estimated using a capacitive tissue model where the material properties were fixed at 1 kHz were found to be similar in shape to previous reported modeling studies [24]. The RMS error of the waveform from the capacitive model with respect to the dispersive model remained above 18% when the material properties were estimated in the range of frequencies between 100 Hz and 2600 Hz, Fig. 4. When the electrical conductivity and the relative permittivity were alternately varied with frequency, higher RMS errors between the capacitive and full dispersive waveforms resulted when dispersion was removed in the relative permittivity than when dispersion was removed in the electrical conductivity, Fig. 5.

The differences in the volume of tissue activated, suggest that a resistive model substantially overestimates the volume of activation, but that a capacitive model with appropriate material properties may provide an approximation to the fully dispersive model, with errors of less than 4.5%, Table II. This is consistent with previous studies where quasi-static solutions were found to overestimate the volume of tissue activated when compared to a capacitive model where material properties were estimated at a single frequency [24]. The volume of tissue activated was underestimated by approximately 58.46% and overestimated by approximately 11.33% when material properties were estimated at 100 Hz and 10 000 Hz respectively. This suggests that estimating material properties at low frequencies leads to underestimation of the volume of tissue activated, and that the use of frequencies above 1 kHz leads to overestimation of the volume of activation.

One of the major limitations of this model, and similar computational models, is the variability that exists in the range of material properties reported in the literature and the accuracy of available dispersive curves [12]. The model presented does not consider local tissue anisotropies, such as in grey matter, nor does it include alternative return current paths caused by areas filled by cerebrospinal fluid [14], [32], which may affect the volume of tissue activated across all tissue models. The composition, dimensions and material properties of the electrode encapsulation region also vary considerably among different studies and have been shown to change with time [7], [14]. This study has considered an idealized whole-head geometry, however the model presented could also be applied to more detailed subject-specific head geometries which have been developed for use in other fields [33]. The over-potential independent formulation was used for the double-layer, neglecting its behaviour at high current densities [30], the consequential difference in the electrode impedance and additional voltage drops which may affect the stimulus delivered to the tissue across all models. Although the double-layer parameters were found to yield lumped impedance values close to experimental values, variations in the electrode and tissue composition may cause these parameters to change, affecting the behaviour of the interface. This study neglects edge effects, which have been shown to increase the current density at the towards the edges of the stimulating contact, and have been shown to be capable of influencing the estimated volume of tissue activated [34], [35]. The lack of anisotropy in the tissue properties may lead to an over-estimation of the volume of tissue activated. The axon orientation has been simplified to align with one of the principal axes, similar to previous studies [6], [14], [35]. Alternative orientations may be expected to result in changes to the estimated volume of tissue activated. Finally the stimuli do not incorporate non-idealities in the output waveform of currently used stimulators [36].

In this study a finite element method of approximating dispersive solutions in arbitary inhomogeneous volume conductors was presented. Although dispersive time-domain solutions for the electric field in finite element models have been developed [37], implementations are not currently available. Furthermore, finite-difference time domain methods are unsuitable for use at the relatively low frequencies typical of bioelectric models [38]. It was therefore necessary to adopt a frequency domain approach as described here. The method presented allows dispersion to be modeled in conjunction with standard finite element analysis techniques. Therefore, it is possible to incorporate features such as thin-layer distributed impedances, irregular geometry, current and voltage inputs and inhomogeneous material properties within a single numerical model. Although this study is presented with application to DBS, the model developed could be used in other applications of volume conductor models in biological tissues in which the incorporation of dispersive material properties is required.

V. Conclusion

In this study the effect of dispersion in material properties on the volume conducted voltage waveforms observed and volume of tissue activated was examined using an inhomogeneous finite element model. The accuracy of capacitive approximations to full dispersive solutions for estimating voltage waveforms and volumes of activation was found to be highly sensitive to the frequency at which material properties were estimated The RMS error of waveforms estimated using capacitive models compared to full dispersive models were found to be in the range of 18% to 95% where material properties were estimated in the range 100 Hz to 2600 Hz. Estimating material properties at lower frequencies were found to cause underestimation of the volume of tissue activated to occur. When material properties at 1 kHz were used, the error in the volume of tissue activated by capacitive approximations was reduced to -4.33% and 11.10% respectively for current-controlled and voltage-controlled stimulation.

Acknowledgements

The authors would like to thank Professor Cameron C. McIntyre of the Cleveland Clinic Foundation, Case Western Reserve University, Cleveland, Ohio, United States for providing the axon model used in this study.

References

[1] K. Ashkan, B. Wallace, B. A. Bell, and A. L. Benabid, "Deep brain stimulation of the subthalamic nucleus in parkinson's disease 1993-2003: where are we 10 years on?" *Br J Neurosurg*, vol. 18, no. 1, pp. 19–34, 2004.

[2] C. C. McIntyre, M. Savasta, B. L. Walter, and J. L. Vitek, "How does deep brain stimulation work? present understanding and future questions." *J Clin Neurophysiol*, vol. 21, no. 1, pp. 40–50, 2004.

[3] J. Volkmann, J. Herzog, F. Kopper, and G. Deuschl, "Introduction to the programming of deep brain stimulators." *Mov Disord*, vol. 17 Suppl 3, pp. S181–7, 2002.

[4] C. C. McIntyre, A. M. Frankenmolle, J. Wu, A. M. Noecker, and J. L. Alberts, "Customizing deep brain stimulation to the patient using computational models," in *Engineering in Medicine and Biology Society, 2009. EMBC 2009. Annual International Conference of the IEEE*, Sept. 2009, pp. 4228–4229.

[5] C. C. McIntyre, A. G. Richardson, and W. M. Grill, "Modeling the excitability of mammalian nerve fibers: influence of afterpotentials on the recovery cycle." *J Neurophysiol*, vol. 87, no. 2, pp. 995–1006, Feb 2002.

[6] C. R. Butson and C. C. McIntyre, "Role of electrode design on the volume of tissue activated during deep brain stimulation." *J Neural Eng*, vol. 3, no. 1, pp. 1–8, 2006.

[7] W. M. Grill and J. T. Mortimer, "Electrical properties of implant encapsulation tissue." *Ann Biomed Eng*, vol. 22, no. 1, pp. 23–33, Sep 1994.

[8] S. N. Sotiropoulos and P. N. Steinmetz, "Assessing the direct effects of deep brain stimulation using embedded axon models." *J Neural Eng*, vol. 4, no. 2, pp. 107–119, 2007.

[9] C. R. Butson, S. E. Cooper, J. M. Henderson, and C. C. McIntyre, "Patient-specific analysis of the volume of tissue activated during deep brain stimulation." *Neuroimage*, vol. 34, no. 2, pp. 661–670, 2007.

[10] P. F. Grant and M. M. Lowery, "Electric field distribution in a finite-volume head model of deep brain stimulation," *Med Eng Phys*, vol. 31, no. 9, pp. 1095–103, Nov 2009.

[11] G. Walckiers, B. Fuchs, J.-P. Thiran, J. R. Mosig, and C. Pollo, "Influence of the implanted pulse generator as reference electrode in finite element model of monopolar deep brain stimulation," *J Neurosci Methods*, vol. 186, no. 1, pp. 90–6, Jan 2010.

[12] S. Gabriel, R. W. Lau, and C. Gabriel, "The dielectric properties of biological tissues: III. parametric models for the dielectric spectrum of tissues." *Phys Med Biol*, vol. 41, no. 11, pp. 2271–2293, 1996.

[13] R. Plonsey and D. B. Heppner, "Considerations of quasi-stationarity in electrophysiological systems." *Bull Math Biophys*, vol. 29, no. 4, pp. 657–664, 1967.

[14] N. Yousif and X. Liu, "Investigating the depth electrode-brain interface in deep brain stimulation using finite element models with graded complexity in structure and solution." *J Neurosci Methods*, Jul 2009.

[15] C. A. Bossetti, M. J. Birdno, and W. M. Grill, "Analysis of the quasi-static approximation for calculating potentials generated by neural stimulation." *J Neural Eng*, vol. 5, no. 1, pp. 44–53, 2008 Mar.

[16] Medtronic, Inc., *Medtronic Activa 37612 implant manual*, Medtronic Inc., Minneapolis, MN, USA, 2009.

[17] P. F. Grant and M. M. Lowery, "Effects of the electrical double layer and dispersive tissue properties in a volume conduction model of deep brain stimulation," *Conf Proc IEEE Eng Med Biol Soc*, vol. 1, pp. 6497–500, 2009.

[18] Y. Eshel, S. Witman, M. Rosenfeld, and S. Abboud, "Correlation between skull thickness asymmetry and scalp potential estimated by a numerical model of the head." *IEEE Trans Biomed Eng*, vol. 42, no. 3, pp. 242–249, 1995.

[19] Medtronic, Inc., *3387-3389 Lead Kit for Deep Brain Stimulation - Implant Manual*, Minneapolis, MA, 2006.

[20] S. Miocinovic, S. Lempka, G. Russo, C. Maks, C. Butson, K. Sakaie, J. Vitek, and C. McIntyre, "Experimental and theoretical characterization of the voltage distribution generated by deep brain stimulation." *Exp Neurol*, 2008 Dec 11.

[21] R. Merwa, K. Hollaus, B. Oszkar, and H. Scharfetter, "Detection of brain oedema using magnetic induction tomography: a feasibility study of the likely sensitivity and detectability." *Physiol Meas*, vol. 25, no. 1, pp. 347–354, 2004.

[22] D. R. Cantrell, S. Inayat, A. Taflove, R. S. Ruoff, and J. B. Troy, "Incorporation of the electrode-electrolyte interface into finite-element models of metal microelectrodes." *J Neural Eng*, vol. 5, no. 1, pp. 54–67, 2008.

[23] A. Richardot and E. T. McAdams, "Harmonic analysis of low-frequency bioelectrode behavior." *IEEE Trans Med Imaging*, vol. 21, no. 6, pp. 604–612, 2002 Jun.

[24] C. R. Butson and C. C. McIntyre, "Tissue and electrode capacitance reduce neural activation volumes during deep brain stimulation." *Clin Neurophysiol*, vol. 116, no. 10, pp. 2490–2500, 2005.

[25] J. Holsheimer, E. A. Dijkstra, H. Demeulemeester, and B. Nuttin, "Chronaxie calculated from current-duration and voltage-duration data." *J Neurosci Methods*, vol. 97, no. 1, pp. 45–50, 2000.

[26] J. Jin, *The Finite Element Method in Electromagnetics*. Wiley-Interscience, 2002.

[27] C. C. McIntyre and W. M. Grill, "Extracellular stimulation of central neurons: influence of stimulus waveform and frequency on neuronal output." *J Neurophysiol*, vol. 88, no. 4, pp. 1592–1604, 2002 Oct.

[28] C. C. McIntyre, W. M. Grill, D. L. Sherman, and N. V. Thakor, "Cellular effects of deep brain stimulation: model-based analysis of activation and inhibition." *J Neurophysiol*, vol. 91, no. 4, pp. 1457–1469, 2004.

[29] M. L. Hines and N. T. Carnevale, "The neuron simulation environment," *Neural Comput*, vol. 9, no. 6, pp. 1179–209, Aug 1997.

[30] X. F. Wei and W. M. Grill, "Impedance characteristics of deep brain stimulation electrodes in vitro and in vivo," *J Neural Eng*, vol. 6, no. 4, p. 046008, Aug 2009.

[31] N. Yousif, R. Bayford, and X. Liu, "The influence of reactivity of the electrode-brain interface on the crossing electric current in therapeutic deep brain stimulation." *Neuroscience*, vol. 156, no. 3, pp. 597–606, 2008 Oct 15.

[32] J. B. J. Ranck and S. L. BeMent, "The specific impedance of the dorsal columns of the cat: an inisotropic medium." *Exp Neurol*, vol. 11, pp. 451–463, 1965.

[33] D. van't Ent, J. C. de Munck, and A. L. Kaas, "A fast method to derive realistic bem models for e/meg source reconstruction." *IEEE Trans Biomed Eng*, vol. 48, no. 12, pp. 1434–1443, 2001 Dec.

[34] X. F. Wei and W. M. Grill, "Current density distributions, field distributions and impedance analysis of segmented deep brain stimulation electrodes." *J Neural Eng*, vol. 2, no. 4, pp. 139–147, 2005.

[35] N. Yousif, N. Purswani, R. Bayford, D. Nandi, P. Bain, and X. Liu, "Evaluating the impact of the deep brain stimulation induced electric field on subthalamic neurons: A computational modelling study," *J Neurosci Methods*, Jan 2010.

[36] C. R. Butson and C. C. McIntyre, "Differences among implanted pulse generator waveforms cause variations in the neural response to deep brain stimulation." *Clin Neurophysiol*, vol. 118, no. 8, pp. 1889–1894, 2007.

[37] N. S. Stoykov, T. A. Kuiken, M. M. Lowery, and A. Taflove, "Finite-element time-domain algorithms for modeling linear debye and lorentz dielectric dispersions at low frequencies." *IEEE Trans Biomed Eng*, vol. 50, no. 9, pp. 1100–1107, 2003.

[38] A. Taflove and S. Hagness, *Computational electrodynamics: the finite-difference time domain method*. Artech House, Inc, 2000.

Peadar F. Grant received the B.E. degree from the School of Electrical, Electronic and Mechanical Engineering, University College Dublin, National University of Ireland, Dublin, Ireland in 2006. He is a student member of the IEEE. He is a postgraduate student with the School of Electrical, Electronic and Mechanical Engineering at University College Dublin, National University of Ireland, Dublin, Ireland. His principal research interest is the computational modelling of deep brain stimulation.

Dr. Madeleine M. Lowery received the B.E. and Ph.D. degrees from the Department of Electronic and Electrical Engineering, University College Dublin, in 1996 and 2000, respectively. Between 2000 and 2005 she held an appointment as a post-doctoral fellow, then Research Scientist and Research Assistant Professor at the Rehabilitation Institute of Chicago and the Department of Physical Medicine and Rehabilitation, Northwestern University. She is currently a Senior Lecturer in the School of Electrical, Electronic and Mechanical Engineering, University College Dublin. She is a member of the IEEE and a member of the council of the International Society of Electrophysiology and Kinesiology. Her research involves exploring nerve and muscle activity through mathematical modelling, analysis and experimentation in order to improve understanding of neuromuscular activity in healthy and diseased states and develop novel and improved rehabilitation strategies. Specific areas of interest include electromyography (EMG), bioelectromagnetics, myoelectric control of artificial limbs, electrical stimulation and neural control of movement.